Whole-field five-dimensional fluorescence microscopy combining lifetime and spectral resolution with optical sectioning

J. Siegel, D. S. Elson, S. E. D. Webb, D. Parsons-Karavassilis, S. Lévêque-Fort, M. J. Cole, M. J. Lever, and P. M. W. French

Femtosecond Optics Group, Department of Physics, and Department of Biological and Medical Systems, Imperial College of Science, Technology and Medicine, Prince Consort Road, London SW7 2BW, UK

M. A. A. Neil, R. Juŝkaitis, L. O. Sucharov, and T. Wilson

Department of Engineering Science, University of Oxford, Parks Road, Oxford OX1 3PJ, UK

Received March 12, 2001

We report a novel whole-field three-dimensional fluorescence lifetime imaging microscope that incoporates multispectral imaging to provide five-dimensional (5-D) fluorescence microscopy. This instrument, which can acquire a 5-D data set in less than a minute, is based on potentially compact and inexpensive diode-pumped solid-state laser technology. We demonstrate that spectral discrimination as well as optical sectioning minimize artifacts in lifetime determination and illustrate how spectral discrimination improves the lifetime contrast of biological tissue. © 2001 Optical Society of America

OCIS codes: 180.0180, 180.2520, 170.0170, 170.6920.

Fluorescence is widely used in biomedicine and other applications to track specific fluorophores and to study anatomical features. Fluorescence lifetime measurements add functional information because they are dependent on the local fluorophore environment (e.g., pO_2, $[Ca^{2+}]$, pH).[1] Fluorescence lifetime imaging (FLIM) is particularly exciting since it can therefore provide noninvasive functional (diagnostic) imaging. Although fluorescence lifetime is more commonly measured in the frequency domain,[2] recent advances in ultrafast gated optical intensifiers and diode-pumped ultrafast lasers make time-domain systems widely deployable.[3,4]

For FLIM it is preferable to resolve the measured fluorescence signal in all three spatial dimensions because out-of-focus light emitted from deeper layers of the sample can lead to a reduction of signal contrast and incorrect lifetime values.[5] Although three-dimensional (3-D) resolution can be achieved by confocal or two-photon excitation techniques, acquiring 3-D lifetime data can be time consuming because the object is scanned pixel by pixel. This drawback can be reduced through the use of multifocal excitation.[6,7] An alternative, nonscanning approach based on structured illumination requires the acquisition of only three whole-field images and has been applied to optical microscopy[8] and recently to FLIM.[9]

Functional information that is complementary to lifetime data can be obtained through spectral resolution.[10] Although both approaches have been combined for single-point measurements,[11] to date, lifetime and spectrally resolved fluorescence images have been acquired separately. To minimize cost and complexity, it is desirable to acquire 3-D lifetime and spectral information with a single imaging detector, which may be realized with a multispectral imager[12] (MI). This provides multiple spectrally resolved images (on a single detector) of a single spatial region. A MI was previously applied to fluorescence intensity imaging.[10] In this Letter we report, for what is to our knowledge the first time, the combination of depth-resolved FLIM and multispectral imaging to realize five-dimensional (5-D) fluorescence imaging with a single imaging detector.

The experimental apparatus is shown in Fig. 1. The laser system comprises a homebuilt diode-pumped Kerr-lens mode-locked Cr:LiSAF oscillator (2×500 mW pump diodes at 670 nm) that seeds a home-built Cr:LiSAF regenerative amplifier (2×500 mW and 1×350 mW pump diodes at 670 nm). The amplified output pulses of ~10-ps duration and 1-μJ energy (at up to 20-kHz repetition rate) are frequency doubled to 430 nm in a BBO crystal for direct excitation of the sample. The resulting fluorescence is imaged onto the entrance plane (image plane 1) of the MI. A dichroic beam splitter then divides the fluorescence into two wavelength passbands to produce a composite output (image plane 2) comprising two spatially identical images of the sample that differ only in their spectral content. A gated optical image intensifier, placed at image plane 2, produces a time-gated (FWHM, <100 ps) fluorescence intensity image that is relayed to an 8-bit intensified CCD camera. FLIM maps are produced by recording a series of time-gated images (17 in this case) at different delays after excitation and fitting the data for each image pixel to a single exponential decay profile by use of a standard nonlinear-least-squares fitting algorithm. One achieves optical sectioning through structured illumination by imaging a (2-line-pair/mm) grating, placed in the excitation beam, onto the sample and recording sets of time-gated fluorescence images for three transverse positions of the grating.[9] Subsequent processing of these images yields both conventional (unsectioned) and sectioned images and FLIM maps.

0146-9592/01/171338-03$15.00/0

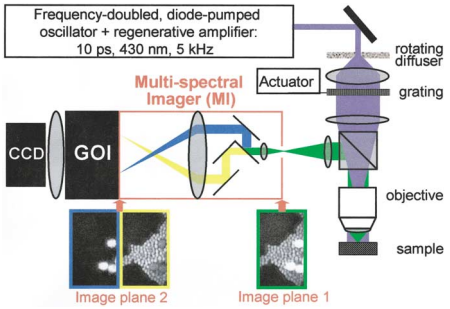

Fig. 1. Experimental setup for whole-field, optically sectioned multispectral fluorescence lifetime imaging. The multispectral imager splits a single image at image plane 1 by its spectral content into two images, spatially identical but with different wavelength bands (image plane 2).

Figure 2(a) shows conventional fluorescence intensity images of 15- and 4.5-μm-diameter fluorescent microspheres (Molecular Probes) imaged at 60× magnification. The MI separates the fluorescence emission above and below 505 nm, which shows the contrast between the two types of microsphere, since they emit at different wavelengths. As a consequence, the larger microspheres appear strongly in the left-hand subimage (450–505 nm) of Fig. 2(a), whereas the smaller microspheres appear on the right (505–800 nm), together with a weaker image of the larger microspheres, whose emission profile extends to this wavelength region. Figure 2(b) shows the corresponding conventional FLIM map for each spectral band. Figures 2(c) and 2(d) show the same fields of view but with the sectioned intensity image pair and corresponding sectioned FLIM maps obtained by use of structured illumination, resulting in a calculated axial sectioning response of 3.1 μm.[8] A comparison of Figs. 2(a) and 2(c) illustrates the improved spatial resolution obtained with sectioning. Even more importantly, Figs. 2(b) and 2(d) illustrate how the out-of-focus light contribution compromises not only the spatial resolution of the FLIM map but also the calculated lifetime values. This is the case for the small spheres located close to the large spheres in the right-hand subimage in Fig. 2(b), which show excessively long lifetime values (red and white areas). The fluorescence decay profile of this region, labeled B in Fig. 2(b), is shown in Fig. 2(e) and exhibits a secondary peak. This secondary emission is pumped by the fluorescence emission of the large spheres, which is more strongly absorbed by the small spheres than the excitation laser radiation. Consequently, the small spheres re-emit this additional energy at their characteristic emission wavelength a significant time (≈1 ns) after the laser-induced fluorescence begins, thereby producing the shoulder in the decay curve and apparently long lifetime values. This phenomenon also affects the lifetime values of the large spheres [C in Fig. 2(b)]. Since the fluorescence intensity recorded at each point in the image is a weighted sum of intensities from all the neighboring points within the 3-D point spread function of the optical system,[5] incorrect lifetime values are obtained wherever the point spread functions of two different fluorophores overlap. The sectioned lifetime map [Fig. 2(d)] is not affected because it shows only the fluorescence that is spatially modulated and thus is insensitive to the secondary emission [Fig. 2(f)].

It is worth noting that only out-of-focus light from different fluorophores leads to lifetime artifacts. This can be seen for the large spheres in region A of Figs. 2(b) and 2(d), which shows almost identical lifetimes [c.f. Figs. 2(e) and 2(f)]. The spectral discrimination is sufficiently strong that the fluorescence contribution from the small spheres is almost negligible (only 5–10 pixel counts out of 256). This result demonstrates that combining spectral discrimination and FLIM can potentially ensure that only single-fluorophore species contribute to a fluorescence lifetime measurement. In the left-hand subimage of Fig. 2(b) the correct lifetime of the large blob, representing out-of-focus light of a 15-μm sphere in a different image plane, is obtained even without optical sectioning; it has the same lifetime value as the in-focus spheres. Appropriate attenuation in the different spectral channels also permits imaging of multiple-fluorophore species with large differences in emission intensity, which would otherwise challenge the dynamic range of the detection.

With a view to investigating the benefit of spectrally resolved FLIM for contrasting biological tissues, we applied the technique to a sample of freshly extracted, unfixed, and unstained rat heart muscle tissue at 10× magnification. In this complex, dense sample the many different endogenous fluorophores that are present cannot be spatially resolved, and optical sectioning is not useful. Multispectral autofluorescence

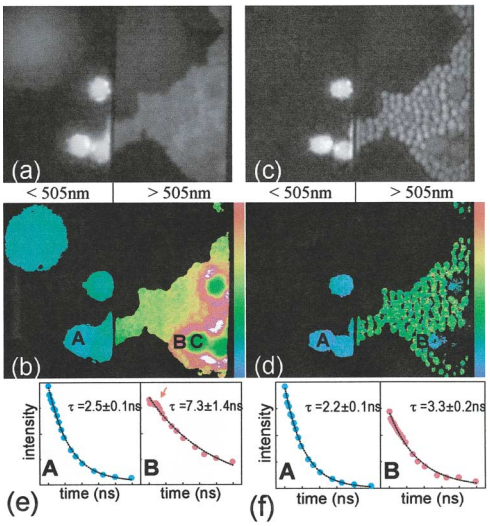

Fig. 2. Spectrally resolved fluorescence image pairs of 15- and 4.5-μm-diameter fluorescent microspheres: (a) conventional and (c) sectioned intensity images and (b) conventional and (d) sectioned FLIM maps. The fluorescence lifetime false-color scale spans 1.5 ns (blue) to 7 ns (pink). Each image pair consists of two spatially identical subimages corresponding to the wavelength bands indicated. The fluorescence decay curves, shown with single-exponential fits in (e) and (f), correspond to the regions marked A and B of FLIM maps (b) and (d), respectively. The red arrow in (e) indicates the peak of the secondary fluorescence emission of the small spheres.

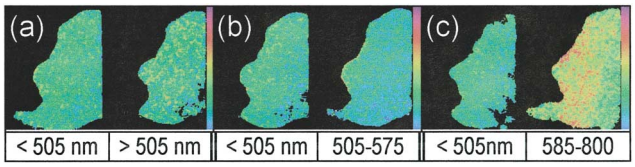

Fig. 3. Spectrally resolved image pairs of (a)–(c) FLIM maps of freshly extracted, unfixed rate heart muscle tissue. The fluorescence lifetime false-color scale spans 0.4 ns (blue) to 1.0 ns (pink).

lifetime imaging, however, can provide additional and more specific tissue contrast by resolving the fluorescence lifetime into wavelength bands. Figure 3(a) shows a FLIM map of a pair of subimages of the tissue sample resolved into the spectral bands indicated. As expected, relatively homogeneous lifetime values are observed over the whole tissue within each image. A small but significant lifetime contrast was observed between the two FLIM subimages, giving values of lifetime τ (<505 nm) = 539 ps and τ (>505 nm) = 554 ps (which we obtained by averaging an area of 50 × 50 pixels at the center of subimage). We attribute this lifetime difference to the presence of different fluorophores. By inserting bandpass filters into the high-pass channel of the spectral imager, we obtained the subimage pairs shown in Figs. 3(b) and 3(c). For the low-pass channel shown on the left in each part of the figure, we obtain consistent lifetimes [Fig. 3(a) 539 ps, Fig. 3(b) 536 ps, Fig. 3(c) 532 ps). This result demonstrates that these values are not changing because of photobleaching and (or) drying of the sample. The right subimages show that for the 585–800-nm emission the lifetime is significantly shorter (486 ps) than for the 505–575-nm emission (663 ps). As expected, the lifetime of the composite emission τ (>505 nm) [Fig. 3(a)] falls between these values. These results illustrate that the observed fluorescence lifetimes in tissue may depend on wavelength, suggesting that combining spectral and temporal resolution to provide a spectral lifetime signature may improve the specificity of fluorescence imaging for biomedicine. We note that, although the standard deviations of the fitted lifetime values obtained are typically ~30 ps, this does not significantly detract from the sensitivity of lifetime contrast between different spectral bands. This is because the deviation from the fit is not caused by a poor signal/noise ratio or random intensity fluctuations but by a deviation from a single-exponential or multiexponential model, as has been suggested to occur in tissue because of interaction between fluorophores and their environment.[13] Nonetheless, the same work shows that the single-exponential model, despite providing a poor fit, is still highly sensitive to lifetime changes.

In summary, we have combined whole-field 3-D FLIM with spectral resolution to achieve 5-D fluorescence microscopy and have realized it by use of compact and relatively inexpensive diode-pumped solid-state laser technology. We have demonstrated how both spectral discrimination and optical sectioning can minimize artifacts in lifetime determination and enhance the information rate in FLIM. We note that rapid 5-D imaging would be invaluable for biochip assays, e.g., for genome sequencing and high-throughput drug screening.[14] We have also shown that enhanced specificity of FLIM in biological tissue can be obtained by proper selection of the studied wavelength band. The spectral resolution (limited in our work to two wavelength bands) can be increased, at the expense of lateral resolution, to as many as eight spectral channels.[12]

The authors gratefully acknowledge the technical advice of Mark Hopkins (Optical Insights). Funding from the UK Engineering and Physical Sciences Research Council (EPSRC), the Biotechnology and Biological Sciences Research Council, and the Paul Instrument Fund of the Royal Society is gratefully acknowledged. D. S. Elson and M. J. Cole acknowledge EPSRC Cooperative Award in Science and Engineering studentships with Kentech Instruments, Ltd., and the Institute of Cancer Research at the ICR/Royal Marsden National Hospital Trust, respectively. S. E. D. Webb and D. Parsons-Karavassilis acknowledge EPSRC studentships.

References

1. J. R. Lakowicz, *Principles of Fluorescence Spectroscopy* (Plenum, New York, 1983).
2. P. C. Schneider and R. M. Clegg, Rev. Sci. Instrum. **68,** 4107 (1997).
3. G. Valentini, C. D'Andrea, D. Comelli, A. Pifferi, P. Taroni, A. Torricelli, R. Cubeddu, C. Battaglia, C. Consolandi, G. Salani, L. Rossi-Bernardi, and G. De Bellis, Opt. Lett. **25,** 1648 (2000).
4. R. Jones, K. Dowling, M. J. Cole, D. Parsons-Karavassilis, M. J. Lever, P. M. W. French, J. D. Hares, and A. K. L. Dymoke-Bradshaw, Electron. Lett. **35,** 256 (1999).
5. A. Squire and P. I. H. Bastiaens, J. Microsc. (Oxford) **193,** 36 (1999).
6. J. Bewersdorf, R. Pick, and S. W. Hell, Opt. Lett. **23,** 655 (1998).
7. A. H. Buist, M. Muller, J. Squier, and G. J. Brakenhoff, J. Microsc. (Oxford) **192,** 217 (1998).
8. M. A. A. Neil, R. Juškaitis, and T. Wilson, Opt. Lett. **22,** 1905 (1997).
9. M. J. Cole, J. Siegel, S. E. D. Webb, R. Jones, K. Dowling, P. M. W. French, M. J. Lever, L. O. D. Sucharov, M. A. A. Neil, R. Juškaitis, and T. Wilson, Opt. Lett. **25,** 1361 (2000).
10. J. Hewett, T. McKechnie, W. Sibbett, J. Ferguson, C. Clark, and M. Padgett, J. Mod. Opt. **47,** 2021 (2000).
11. J.-M. I. Maarek, L. Marcu, M. C. Fishbein, and W. S. Grundfest, Lasers Surg. Med. **27,** 241 (2000).
12. Optical Insights, LLC, Suite 60, 1807 Second Street, Santa Fe, N. Mex. 87505, http://www.optical-insights.com; "Multi-spectral two dimensional imaging spectrometer," U.S. patents 5,926,283 (July 20, 1999) and 5,982,497 (November 9, 1999).
13. K. C. Benny Lee, J. Siegel, S. E. D. Webb, S. Lévêque-Fort, M. J. Cole, R. Jones, K. Dowling, P. M. W. French, and M. J. Lever, Biophys. J. **81,** 1250 (2001).
14. M. V. Rogers, Drug Discovery Today, **2,** 156 (1997).